Optimizing Thermal Management with Regulated Jet Impingement Boiling Cooling and Transverse Airflow: A Parametric Analysis

Guerfi Djamel Eddine[1,2], Roux Stéphane[3], Allanic Nadine[2], Sarda Alain[2], Lecointe Damien[1]
[1]Nantes Université, IRT Jules Verne, F-44000 Nantes, France
djamel-eddine.guerfi@etu.univ-nantes.fr; damien.lecointe@irt-jules-verne.fr
[2]GEPEA Nantes Université, Oniris, CNRS, GEPEA, UMR 6144, F-44000 Nantes, France
nadine.allanic@univ-nantes.fr; alain.sarda@univ-nantes.fr
[3]Nantes Université, CNRS, Laboratoire de Thermique et Energie de Nantes, LTeN, UMR 6607, F-44000 Nantes, France
stephane.roux@univ-nantes.fr

Abstract - In our pursuit of refining water jet impingement boiling cooling with transverse airflow for enhanced thermal management, an extensive experimental investigation has been conducted to assess the influence of key hydraulic and aeraulic parameters on cooling performance. These parameters include air flow rate, jet orientation, jet spacing, and jet diameter, which collectively impact cooling efficiency, temperature control, and uniformity of the upper surface in contact with the manufactured component. Our findings reveal compelling insights: optimizing these parameters led to marked improvements in thermal management, ensuring consistent product quality. Further, cooling regulation mechanisms have been integrated, achieving precise control over the cooling rate. These outcomes hold promising implications for various industrial applications, particularly in shaping thermoplastic matrix composite materials, where precise and uniform cooling is vital for product quality assurance. This research aims to define the optimal jet configuration for more efficient heat dissipation while maintaining precise temperature control and enhanced cooling uniformity. This study offers promising prospects for designing more efficient cooling systems in various industrial applications, thereby contributing to improving manufacturing process performance.

Keywords: - Jet Impingement Boiling - Enhanced Thermal Management - Cooling Regulation - Heat Transfer Optimization Transverse Airflow - Multiphase Flow

1. Introduction

The use of jets for mold cooling is common in many industrial applications [1]–[3]. This technique has proven effective in maintaining optimal temperatures in environments such as the aerospace industry and sheet metal production. However, its application in cooling thermoplastic matrix composite materials presents specific challenges due to high processing temperatures (300-450°C). These temperatures can lead to convective boiling phenomena and cooling inequalities, which can adversely affect the quality of the produced parts [4], [5].

The assessment of heat exchange in the context of cooling by jet impact is an evolving research field. In this context, Devahdhanush et al. [6], [7] provided a comprehensive review of studies addressing the dependence of thermal flux density on jet velocity, total mass flow rate, and jet diameter. Additionally, the work by Lee et al. [8] revealed the importance of an optimal spacing between jets to ensure efficient heat transfer, especially in the overlapping zone during the interaction between adjacent jets. In parallel, Prakash et al. [9] investigated cross-flow of transverse air with water jets, seeking to determine optimal flow conditions based on various flow rate ratios while identifying jet stability thresholds.

Research efforts in our laboratory, initiated by Tymen et al.[10], have focused on visualizing two-phase flow and the distribution of water phases during the cooling of a cylindrical channel heated to 450°C. Their findings underscored the significance of gradients and average vapor volume fractions in heat exchange with the wall. Building upon the research of Agyeman et al. [11], [12], an innovative approach based on boiling induced by impacting jets is introduced. This method combines the use of water jets directed towards the internal mold surface with transverse airflow, aiming to achieve uniform and controlled cooling, with the ultimate goal of improving thermal management for enhanced part quality. Moreover, we seek to evaluate the influence of specific hydraulic and aeraulic parameters, such as mass flow rate ratio, jet orientation, number, spacing and diameter, on the intensity of heat exchange with the cylindrical channel wall, while ensuring compliance with upper surface cooling directives.

2. Experiment and methods

Fig. 1 provides a detailed view of the laboratory's experimental setup, which has been previously described in earlier research conducted in the laboratory [12], along with the network of fluid conduits used in this study. At the core of our experiments lies the test element, a solid block made of 316L stainless steel measuring 200 mm × 100 mm × 90 mm. To ensure optimal thermal insulation throughout the experiments, this block is carefully enveloped in a 30 mm layer of silica wool. The cooling process is meticulously regulated through water jets generated by a central tube carefully coaxially inserted into the drilled channel of the steel block. These water jets are oriented against gravity (0°) to optimize the cooling process. During the experiments, air continues to circulate within the channel to prevent any vapor condensation effects.

To maintain consistent conditions, the ratio of hydraulic diameter ($d_h = 7.5mm$) to jet diameter ($d_j = 1mm$), i.e., (D_h/d_j) is kept constant at 7.5. Additionally, the jet-to-jet spacing ratio (D_j/d_j), representing the distance between jets (D_j) relative to their diameter (d_j), is fixed at 30. Throughout our experiments, we maintain a constant water flow rate ($Q_{wat} = 1.4l/min$), while the Target Cooling Rate (TCR) is held at $15°C/min$.
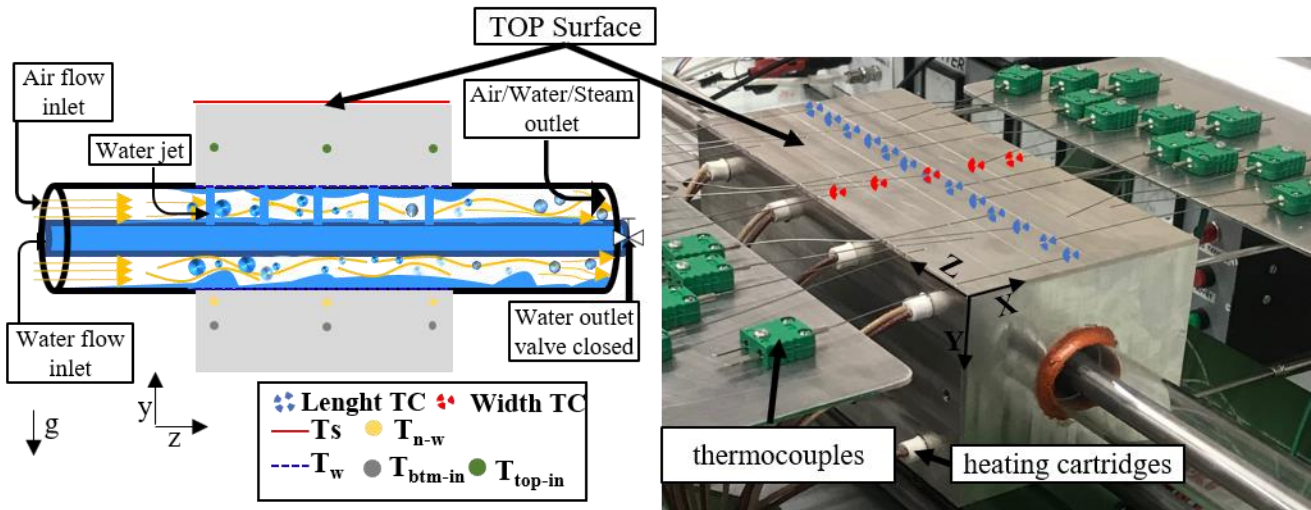

Fig. 1 Cooling principle and Test element description

2.1. Cooling control procedure

The experimental protocol commences by heating the test element to a temperature of 320°C, a process facilitated by 8 heating cartridges. Additionally, a low air flow rate (Q_a) of $14l/min$ is introduced into the annular space between the central tube and the inner surface of the perforated channel in the block Fig. 1. This air injection aims to efficiently evacuate water vapor, thereby preventing its condensation within the channel or in its vicinity. Once the test element is adequately heated, a forced convection cooling process is initiated, employing a moderate air flow rate. This step is designed to ensure uniform heat distribution across the test element's surface until the average temperature reaches the predefined target of 300°C. At this stage, the cooling control algorithm comes into play. This algorithm continuously compares the average temperature of the upper surface of the test element, derived from data collected by 25 thermocouples (Fig. 1) distributed across the surface (Ts), to the Target cooling temperature (TCR). The activation of the cooling actuator, i.e., the opening of the water valve, is thus determined by the difference between the measured average temperature and the TCR The model and the method's principles have been extensively described in previous research conducted at the laboratory [12]. Throughout the entire experiment, an airflow is consistently maintained in the annular space between the tube and the canal wall. The airflow serves several purposes: ensuring a continuous but gradual cooling of the block, even in the absence of water jets; preventing the canal from filling with water during jet impact; and draining any residual water from the canal after the valve closure, as the block would otherwise continue to cool through the boiling of remaining water.

2.2. Quantifying Boiling Heat Transfer Methodology

In order to assess heat transfer within the test element, it is imperative to first quantify these transfers at the level of the wall directly impacted by fluid flows. However, due to the experimental configuration with a cylindrical channel, it is

extremely challenging to precisely measure local wall temperatures. Therefore, we adopted a numerical approach, utilizing the Inverse Heat Conduction Problem (IHCP). This methodology has been previously employed by Twomey [13] and Beck et al. [14] to obtain numerical estimations using the internal temperature distribution recorded on a plate[15].
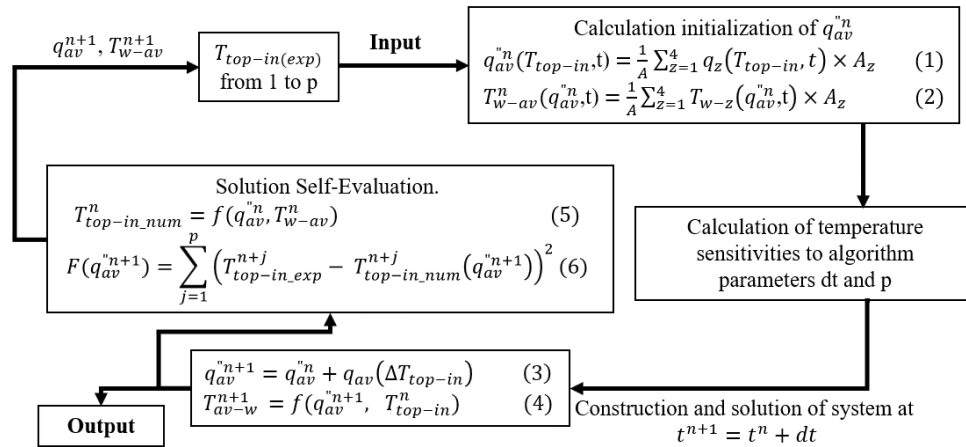

Input

$q_{av}^{n+1}, T_{w-av}^{n+1}$

$T_{top-in(exp)}$ from 1 to p

Calculation initialization of $q_{av}^{"n}$

$q_{av}^{"n}(T_{top-in},t) = \frac{1}{A}\sum_{z=1}^{4} q_z(T_{top-in},t) \times A_z$ (1)

$T_{w-av}^{n}(q_{av}^{"n},t) = \frac{1}{A}\sum_{z=1}^{4} T_{w-z}(q_{av}^{"n},t) \times A_z$ (2)

Solution Self-Evaluation.

$T_{top-in\_num}^{n} = f(q_{av}^{"n}, T_{w-av}^{n})$ (5)

$F(q_{av}^{"n+1}) = \sum_{j=1}^{p}\left(T_{top-in\_exp}^{n+j} - T_{top-in\_num}^{n+j}(q_{av}^{"n+1})\right)^2$ (6)

Calculation of temperature sensitivities to algorithm parameters dt and p

$q_{av}^{"n+1} = q_{av}^{"n} + q_{av}(\Delta T_{top-in})$ (3)

$T_{av-w}^{n+1} = f(q_{av}^{"n+1}, T_{top-in}^{n})$ (4)

Construction and solution of system at $t^{n+1} = t^n + dt$

Output

Fig. 2 Method execution algorithm

As illustrated in Fig. 2, Beck's method relies on calculating each value of the average heat flux density ($q_{av}^{"}$) from experimental measurements of T_{top-in} over a sliding time horizon. Here, T_{top-in} represents the experimental measurements (Fig. 1), p: is the number of future time steps, $q_{av}^{"}$is the average heat flux density over the entire wall, A: is the wall surface area ($0.16m^2$), z: represents the wall zone (stagnation, overlap, Upper and Lower zones[8]), T_{w-av} is the average wall temperature, dt: is the time interval (4 s), and$F$: is the cost function optimized by the method.

Due to the complexity of hydrodynamic interactions of the jets and their state variations when they come into contact with a hot wall, we used jet impingement cooling data from the literature [8], [11], [12]] to impose heterogeneity in the heat flux density for each wall zone, as defined by equations (1) and (2). Equations (3) to (6) outline the calculations necessary to obtain the values of the average heat flux ($q_{av}^{"}$) for each time step.

To evaluate heat exchanges along the wall, we employed the aforementioned IHCP model, which required the execution of a MATLAB© program in conjunction with COMSOL© with finite element method to solve the heat transfer equation (eq7).

$$\rho(T)Cp(T)\frac{\partial T}{\partial t} = \nabla(k(T) \nabla T)$$ (07)

We also considered the non-linearity of the physical properties of steel (density (ρ), specific heat capacity (Cp), thermal conductivity (k)) as functions of temperature, as reported in the literature[16]. Given the presence of a 30 mm thick thermal insulating layer of silica wool with low thermal conductivity, we imposed a relatively low overall heat transfer coefficient as a boundary condition on the outer boundaries of the test element model, to account for thermal losses through conduction across the thermal insulator and natural convection at an external temperature of 20°C.

3. Results and discussion
3.1 Reference case with and without control

A preliminary work has been conducted to assess the impact of method parameters, without flow regulation, on the accuracy of the model. It revealed a degradation in accuracy when the time step exceeded 4 seconds or when the number of future time steps exceeded 5. To ensure optimal precision, we carefully selected ideal values for our calculations, with a time step (dt) of 4 seconds and a number of future time steps (p) equal to 5.

Fig. 3a depicts the response of some thermocouples in different regions of the block, along with a comparison of heat exchanges at the wall level between a reference cooling case with $Q_{wat} = 1.4\ l/min$ and $Q_a = 40 l/min$ for cooling with and without regulation
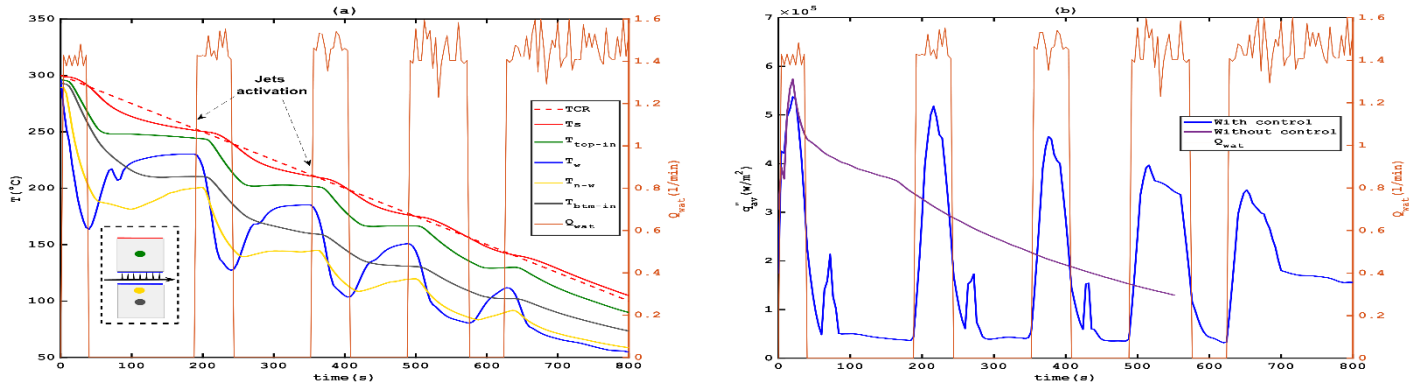
Fig. 3 Typical results for reference case: (a) Thermocouples responses (b) Heat Exchange on the Wall

The curves in Fig. 3 present experimental measurements, including temperatures within the block and on its upper surface. The blue curves in both figures represent numerical results obtained using the inverse method. These figures reveal the activation of water jets as soon as the temperature of the block's upper surface (Ts) exceeds the setpoint temperature TCR. Regarding the response time, the temperature of the wall calculated by the numerical model is in perfect synchrony with the activation of the jets, showing an immediate response with cooling rates reaching *356°C/min* during the first cooling step. This value gradually decreases in the subsequent steps, dropping to *267°C/min* for the second step and *109°C/min* for the fifth step. This reduction is likely due to the decrease in wall temperature and the decrease in heat flux density exchanged with the wall. We also observe that the response time varies: it is 10 seconds for thermocouples close to the wall (Tn-w), 14 to 18 seconds for thermocouples located *15mm* from the wall (T_{top-in} in green and T_{btm-in} in gray), and 28 seconds for thermocouples on the upper surface located *30mm* from the surface impacted by the jets.

To explain the variations in the average heat flux density ($q_{av}^{"}$) exchanged with the wall during regulated cooling, we conducted similar experiments without regulation using the same air (Q_a 40l/min) and water (Q_{wat} 1.4l/min) flow rates. At the first step, we observe a similar behavior before the jets are stopped by the regulation algorithm to limit overshoot relative to the imposed cooling rate. However, we found that discontinuous cooling manages to generate higher heat flux densities when the jets restart, with values ranging from $5.7 \times 10^5 W/m^2$ at the second step to $3.45 \times 10^5 W/m^2$ at the fifth step, compared to a decrease in $q_{av}^{"}$ from $3.19 \times 10^5 W/m^2$ to $1.29 \times 10^5 W/m^2$ in the same temperature range. Another important conclusion from this analysis concerns the peaks in heat flux density that occur in the absence of jet activation. Although their values do not exceed $2.13 \times 10^5 W/m^2$, they represent *34%* of the main peak. This behavior on the wall after the cessation of water flow is due to cooling caused by water vapor resulting from the boiling of remaining water droplets in the cylindrical channel, leading to recondensation.

These two figures, (a) and (b), clearly illustrate the effectiveness of the regulation algorithm in adhering to the prescribed cooling rate (**TCR**) of $15°°C/min$.

3.2 Model Accuracy and Validation of the Numerical Method

To further validate our numerical approach, we begin by comparing the experimental temperature measurements obtained from the T_{top-in} thermocouples, marked in green in Fig. 4, with the temperatures calculated numerically at the same locations, as shown in the self-evaluation phase in Figure 2. Continuing our validation process, we also compare the near-wall temperatures, T_{n-w}, indicated in yellow, obtained using the three thermocouples located *5mm* from the wall, with the values calculated by our model for the same position.
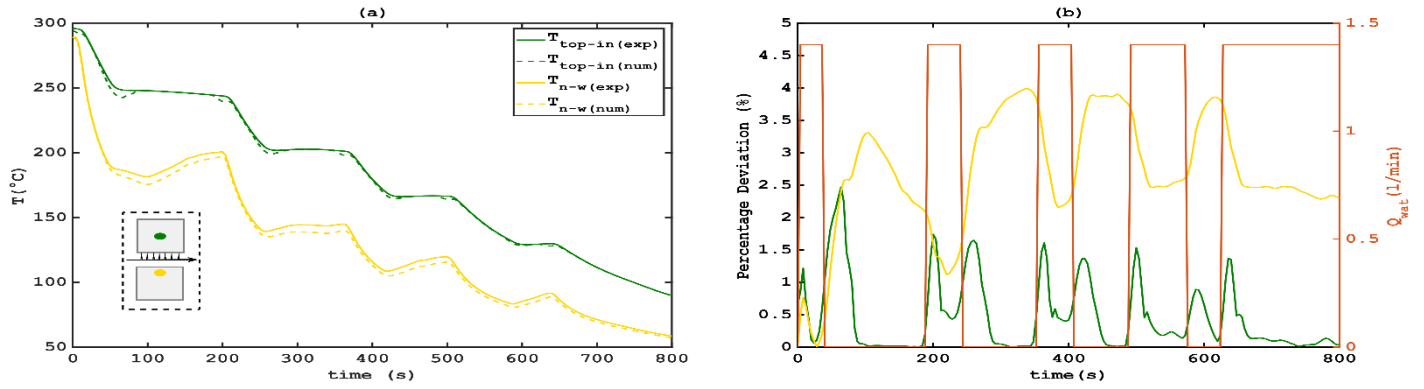
Fig. 4 Accuracy assessment of calculations (a): calculation errors (b): Percentage deviation

These two figures highlight the high precision of our model in predicting temperatures at various distances from the wall, with a Mean Squared Error (*MSE*) of *1.6°C* for the prediction of T_{top-in}T in green, with a percentage error relative to the experimental temperature not exceeding 2.5%, even during jet activation. We observe a slight increase in the error, resulting in an MSE of *3.66°C*, corresponding to a percentage error relative to the experimental temperature not exceeding 4%, for temperatures near the wall (T_{n-w}in yellow), due to the greater distance from the initial model data. It is also worth noting that, in order to eliminate the effect of measurement distance, and in the case of configurations with jets oriented against gravity, we use T_{btm-in}, shown in grey in Fig. 1 , as initial model data to maintain a distance of *15mm* from the jet impact point.

3.3 Influence of flow ratio and jet orientation

In order to investigate the effect of jet flow ratios, we employed two flow configurations with different mass flow rate ratios. Additionally, to assess the influence of jet orientation, in contrast to our reference case where the jets are directed against gravity (0°), we used configurations with jets oriented downward, following gravity (180°). The Tab. 1 below summarizes the values of flow rates, mass flow rate ratios, and Reynolds numbers used in our experiments.:

Tab. 1 Flow Rate Ratios and Reynolds Conditions

Tube	Q_{wat} $(l.min^{-1})$	v_j $(m.s^{-1})$	Re_j	Q_a $(l.min^{-1})$	v_a $(m.s^{-1})$	Re_a	$\dfrac{\dot{m}_j}{\dot{m}_a}$
7 j	1,4	4.25	**4250**	40	2,9	**3500**	4
				350	25,7	**30000**	0,5
4J-1mm		7,5	**7400**	40	2,9	**3500**	7,3
4J-2mm		1.85	**3700**				
19J-1mm		1,5	**1550**				1,5
19J-2mm		0.39	**780**				

The cooling curves of the upper surfaces (Fig. 5a) and the corresponding deviations from the Target Cooling Rate (TCR) (Fig. 5c) demonstrate that reducing the flow rate ratio (σ) improves rate tracking, with a mean squared error (MSE) of 6.5°C over the cooling period *[0-800s]* and a maximum deviation of 19°C, compared to an MSE of *7.1°C* and a maximum deviation of 22°C. However, orienting the jets downward, in the direction of gravity, significantly impairs rate tracking, with an MSE increasing from *6.5°C* to *9.4°C* for high airflows. Regarding heat exchange at the wall level Fig. 5b the flow rate ratio has an almost negligible effect when flows are oriented against gravity. However, with low airflows and downward-oriented jets, a substantial deterioration in heat exchange is observed. This can be attributed to the uneven distribution of the wetted area on the wall. When jets are oriented against gravity, the gravitational force helps efficiently remove water from the jets towards the exit of the channel, promoting a uniform distribution of wall cooling and reducing residual vaporization. This hypothesis is supported by the absence of secondary peaks in the heat flux density curves during low airflow cooling oriented downward (dashed red curve Fig. 5b).
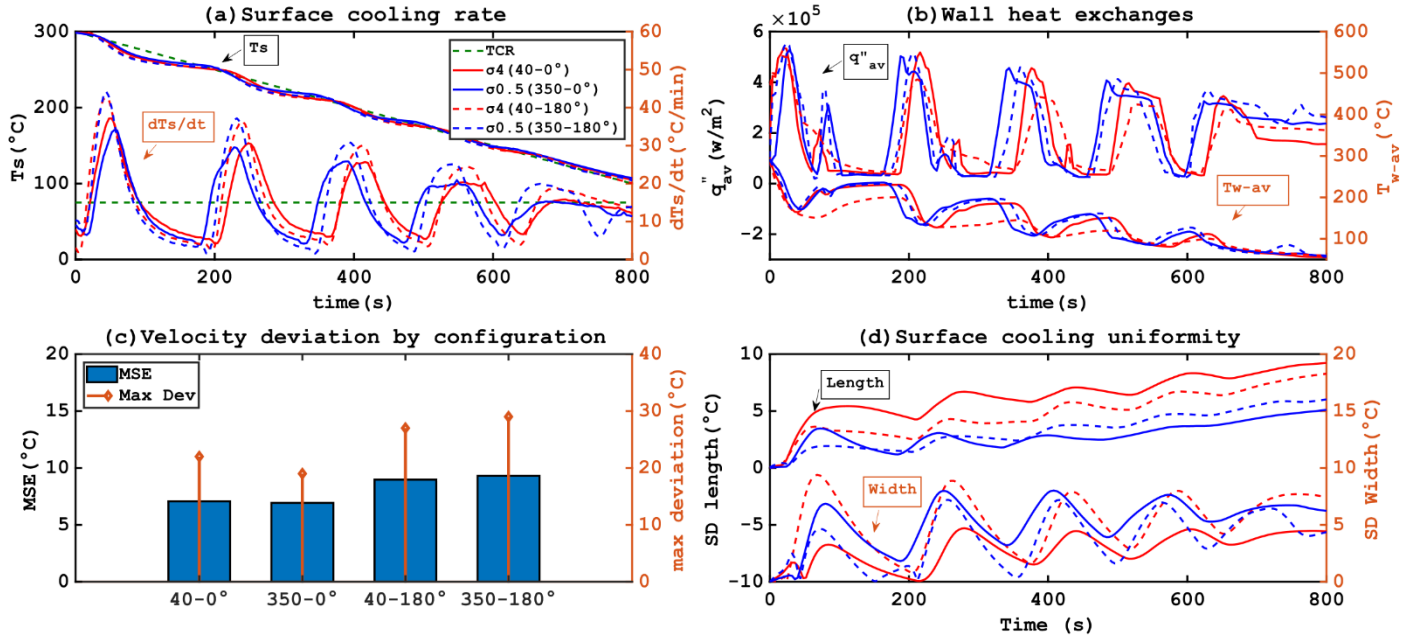
Fig. 5 Influence of flow ratio and jets orientation

To assess the uniformity of temperature on the upper surface of the test element, both longitudinally and laterally (see Fig. 1), we used the standard deviation, calculated using equations 6. The recorded temperatures over time were adjusted to eliminate temperature variations at the beginning of cooling. The standard deviation allows us to quantify temperature variations from the mean, providing information on temperature fluctuations.

$$SD(t) = \sqrt{\frac{\sum_{i=1}^{n} |E_i(t) - \bar{E}_i(t)|^2}{x-1}} \tag{8}$$

Where $\bar{E}(t)$ is the average of $(E_i(t))_{i \in [1,n]}$, n: Number of thermocouples; x = number of computed differences (78 for length and 10 for width) . $t_{final} = 800$ s, $dt = 2s$

Our analyses of Fig. 5d, reveal that the uniformity of cooling varies depending on the cycles of jet activation and deactivation, facilitating heat transfer between hot and cold zones. A reduction in the flow ratio (σ), along with increased airflow, improves uniformity along the upper surface, reducing the average standard deviation (SD_{av}) from *6.4°C* to *2.8°C*. However, across the width of the block, SD_{av} increases from 2.8°C to 5.2°C with increased airflow. The orientation of the jets in the direction of gravity (180°), with a reduced cooling rate, eliminates the effect of air ratio, reducing SD_{av} from *4.8°C* to *3.3°C* longitudinally and from *5.2°C* to *3.8°C* laterally.

3.4 Influence of the size and distribution of water jets

When the diameter of the jets is increased to 2 mm, the D_h/d_j ratio becomes 3.75, and the jet spacing ratio, D_j/d_j, will be 15. The influence of the number of jets and their diameters on the cooling regulation is illustrated in Fig. 6.

The analysis of the influence of these two parameters presented in Fig. 6 reveals that cooling with a tube of 7 jets significantly improves tracking of the setpoint. This observation is in line with our previous experiments without cooling regulation, and it is also consistent with what has been mentioned in the literature [7]. It emphasizes that an optimal value for the number of jets allows our SEC to cool more effectively by avoiding excessive proximity or distance between the jets, which promotes a more even distribution of wall cooling. This results in a reduction of the Mean Squared Error (MSE) from *11°C* to *7°C* and a reduction of the maximum deviation from *33°C* to *20°C* with an average number of jets. These conclusions also apply to heat exchange at the wall, where increasing the number of jets does not increase the intensity of heat exchange in any way.
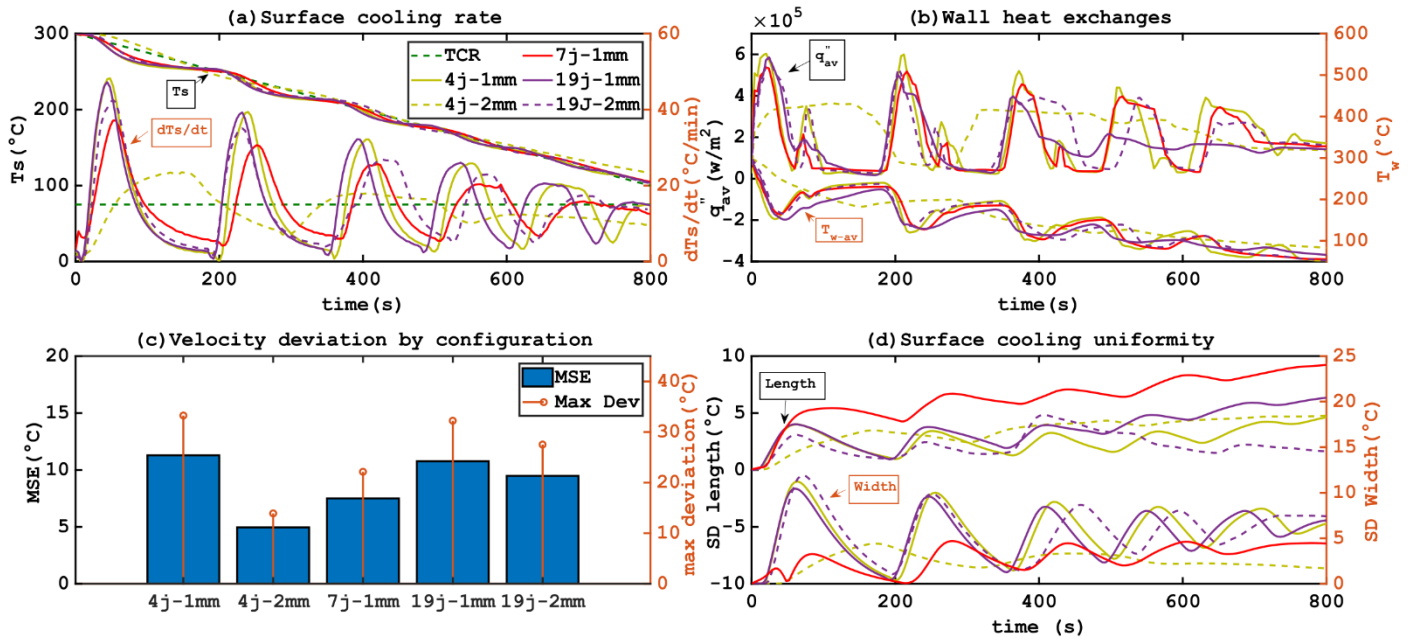
Fig. 6 Influence of distance and diameter of jets

As for the effect of changing the diameter, which significantly affects jet velocity, we observe that reducing jet velocity allows our SEC to better track the setpoint, reducing the MSE from *11°C* to *4.9°C* for 4-jet tubes and from *9°C* to *4.9°C* for 19-jet tubes. This improvement is due to the slowed cooling resulting from reduced jet velocities. Given that our imposed velocity is *15°C/min*, using lower jet velocities is better suited to this type of cooling. However, if the imposed TCR exceeds *20°C/min,* the effect is reversed, and our SEC can no longer follow the imposed TCR setpoint, as previously observed with unregulated flows. The heat exchange curves at the wall confirm these observations, showing a significant loss of heat exchange intensity with larger diameters, decreasing from *482°C/min* to *100°C/min* for 4-jet tubes, with a less pronounced effect for 19-jet tubes, proportional to the difference in jet velocities.

Regarding homogeneity in Fig. 6d , although the configuration with 7 jets improves homogeneity along the length of the inner wall, it does not have this advantage on the upper surface. On the other hand, increasing the diameter reduces the cooling rate, improving homogeneity in width and on the upper surface (SD_{av} decreases from *5.6°C* to *2.4°C*). The results suggest complexity in the relationship between flow parameters and cooling homogeneity. It should be noted that the shape of the curve for the 7-jet configuration in Fig. 6d is primarily due to the position of the reference line in width, coinciding exactly with the central jet of the 7-jet configuration, allowing for better cooling of this line. However, this does not imply in any way that this configuration results in superior homogeneity in width on the upper surface, as the improvement of this criterion is directly related to the position of the jets and the cooling rate.

4. Conclusion

This in-depth study of cooling mechanisms within the context of thermal regulation via impinging jets has yielded several crucial findings. Drawing from the numerous parameters examined in this research, the following key points can be highlighted:

Precise Experimental Configuration: The meticulously calibrated experimental setup, characterized by a different hydraulic diameter (D_h/d_j) and defined jet spacing (D_j/d_j) , provided a solid foundation for the thorough analysis of heat exchange and Critical Heat Flux (CHF) distribution in our impinging jet cooling system with transverse airflow. These consistent conditions were essential for this study.

Modeling Method: A numerical approach based on the Inverse Heat Conduction Problem (IHCP) was adopted to quantify heat transfers at the wall impacted by fluid flows. This method proved to be accurate, with remarkable comparisons between experimental data and numerical results.

Regulation Efficiency: This research demonstrated the effectiveness of the regulation algorithm in maintaining the imposed cooling rate (TCR) of *15°C/min*, ensuring precise control of the cooling process. Synchronized response times with jet activation were particularly noteworthy, even when cooling rates varied.

Impact of Flow Parameters: The orientation of jets relative to gravity, the flow rate ratio (σ), and jet diameter all showed significant influence on cooling performance. For example, jets oriented against gravity favored even cooling distribution, while smaller jet diameters enabled better temperature setpoint tracking.

Cooling Uniformity: Temperature uniformity on the upper surface of the test element was extensively evaluated. Results demonstrated variations in uniformity depending on parameters, with longitudinal gains in uniformity and lateral losses, depending on jet orientation and flow rate ratio.

In summary, this research has contributed to a better understanding of impinging jet cooling mechanisms while identifying optimization opportunities to ensure efficient and uniform thermal management. These findings offer promising prospects for designing more effective cooling systems in various industrial applications, particularly in the field of thermoplastic matrix composite materials, where precise temperature control is essential for ensuring product quality. The ongoing commitment to addressing these cooling challenges will contribute to improvements in industrial manufacturing processes.

Acknowledgements

References

[1] L. Yi, H. Hu, C. li, Y. Zhang, S. Yang, et M. Pan, « Experimental investigation on enhanced flow and heat transfer performance of micro-jet impingement vapor chamber for high power electronics », *International Journal of Thermal Sciences*, vol. 173, p. 107380, 2022

[2] Y. Cheng, A. A. O. Tay, et X. Hong, « An experimental study of liquid jet impingement cooling of electronic components with and without boiling », in *Advances in Electronic Materials and Packaging 2001 (Cat. No.01EX506)*, nov. 2001, p. 369-375.

[3] R. D. Plant, J. Friedman, et M. Z. Saghir, « A review of jet impingement cooling », *International Journal of Thermofluids*, vol. 17, p. 100312, 2023.

[4] A. Agazzi, V. Sobotka, R. LeGoff, et Y. Jarny, « Optimal cooling design in injection moulding process – A new approach based on morphological surfaces », *Applied Thermal Engineering*, vol. 52, nᵒ 1, p. 170-178, 2013.

[5] T.-H. Wang et W.-B. Young, « Study on residual stresses of thin-walled injection molding », *European Polymer Journal*, vol. 41, nᵒ 10, p. 2511-2517, 2005.

[6] V. S. Devahdhanush et I. Mudawar, « Review of Critical Heat Flux (CHF) in Jet Impingement Boiling », *International Journal of Heat and Mass Transfer*, vol. 169, p. 120893, 2021.

[7] V. S. Devahdhanush et I. Mudawar, « Critical Heat Flux of Confined Round Single Jet and Jet Array Impingement Boiling », *International Journal of Heat and Mass Transfer*, vol. 169, p. 120857, 2021.

[8] S. G. Lee, M. Kaviany, et J. Lee, « Quench subcooled-jet impingement boiling: Two interacting-jet enhancement », *International Journal of Heat and Mass Transfer*, vol. 126, p. 1302-1314, 2018.

[9] R. Surya Prakash, A. Sinha, G. Tomar, et R. V. Ravikrishna, « Liquid jet in crossflow – Effect of liquid entry conditions », *Experimental Thermal and Fluid Science*, vol. 93, p. 45-56, 2018.

[10] G. Tymen , N. Allanic, A. Sarda, P. Mousseau, C. Plot, Y. Madec et J.P. Caltagirone , « Temperature mapping in a two-phase water-steam horizontal flow », *Experimental Heat Transfer*, vol. 31, nᵒ 4, p. 317-333, 2018.

[11] E. Agyeman, D. Edelin, et D. Lecointe, « Experimental Study of the Effect of a Cross Airflow on the Dynamics and Heat Transfer Performance of Impinging Circular Water Jets on a Concave Surface », *Heat Transfer Engineering*, 2021.

[12] E. Agyeman, P. Mousseau, A. Sarda, D. Edelin, et D. Lecointe, « Homogeneous and automated cooling of a mould segment by multiple water jet impingement and a cross air flow », *Journal of Thermal Science and Engineering Applications*, 2021.

[13] S. Twomey, « The application of numerical filtering to the solution of integral equations encountered in indirect sensing measurements », *Journal of the Franklin Institute*, vol. 279, nᵒ 2, p. 95-109, 1965.

[14] J.V. Beak, B. Blackwell, C.R. St. Clair, Inverse Heat Conduction, Wiley, New York,1985

[15] S. G. Lee, M. Kaviany, C.-J. Kim, et J. Lee, « Quasi-steady front in quench subcooled-jet impingement boiling: Experiment and analysis », *International Journal of Heat and Mass Transfer*, vol. 113, p. 622-634, 2017.

[16] C. S. Kim, « Thermophysical properties of stainless steels », Argonne National Lab., Ill. (USA), ANL-75-55, sept. 1975.